Polarization transfer in Rayleigh scattering of hard x-rays

2016 New J. Phys. 18 103034

(http://iopscience.iop.org/1367-2630/18/10/103034)

New Journal of Physics
The open access journal at the forefront of physics

Deutsche Physikalische Gesellschaft DPG
IOP Institute of Physics

Published in partnership with: Deutsche Physikalische Gesellschaft and the Institute of Physics

OPEN ACCESS

RECEIVED
8 August 2016

REVISED
21 September 2016

ACCEPTED FOR PUBLICATION
26 September 2016

PUBLISHED
20 October 2016

PAPER

Polarization transfer in Rayleigh scattering of hard x-rays

K-H Blumenhagen[1,2,3], S Fritzsche[1,4], T Gassner[1,2,3], A Gumberidze[2,5], R Märtin[1,2], N Schell[6], D Seipt[1], U Spillmann[2], A Surzhykov[7,8], S Trotsenko[1,2], G Weber[1,2], V A Yerokhin[1,9] and T Stöhlker[1,2,3]

[1] Helmholtz-Institut Jena, Fröbelstieg 3, D-07743 Jena, Germany
[2] GSI Helmholtzzentrum für Schwerionenforschung GmbH, Planckstraße 1, D-64291 Darmstadt, Germany
[3] Institut für Optik und Quantenelektronik, Friedrich-Schiller-Universität Jena, Max-Wien-Platz 1, D-07743 Jena, Germany
[4] Theoretisch-Physikalisches Institut, Friedrich-Schiller-Universität Jena, Fröbelstieg 1, D-07743 Jena, Germany
[5] ExtreMe Matter Institute EMMI, GSI Helmholtzzentrum für Schwerionenforschung, Planckstraße 1, D-64291 Darmstadt, Germany
[6] Helmholtz-Zentrum Geesthacht-Zentrum für Material- und Küstenforschung GmbH, Max-Planck-Straße 1, D-21502 Geesthacht, Germany
[7] Physikalisch-Technische Bundesanstalt, Bundesallee 100, D-38116 Braunschweig, Germany
[8] Technische Universitt Braunschweig, Pockelsstraße. 14, D-38106 Braunschweig, Germany
[9] Center for Advanced Studies, Peter the Great St. Petersburg Polytechnic University, Polytekhnicheskaya 29, 195251 St. Petersburg, Russia

E-mail: k.-h.blumenhagen@gsi.de

Keywords: Rayleigh scattering, x-ray scattering, x-ray polarimetry

Abstract

We report on the first elastic hard x-ray scattering experiment where the linear polarization characteristics of both the incident and the scattered radiation were observed. Rayleigh scattering was investigated in a relativistic regime by using a high-Z target material, namely gold, and a photon energy of 175 keV. Although the incident synchrotron radiation was nearly 100% linearly polarized, at a scattering angle of $\theta = 90^\circ$ we observed a strong depolarization for the scattered photons with a degree of linear polarization of $+0.27\% \pm 0.12\%$ only. This finding agrees with second-order quantum electrodynamics calculations of Rayleigh scattering, when taking into account a small polarization impurity of the incident photon beam which was determined to be close to 98%. The latter value was obtained independently from the elastic scattering by analyzing photons that were Compton-scattered in the target. Moreover, our results indicate that when relying on state-of-the-art theory, Rayleigh scattering could provide a very accurate method to diagnose polarization impurities in a broad region of hard x-ray energies.

1. Introduction

Elastic scattering of hard x-rays by atoms is a fundamental process which is usually described as a coherent sum of scattering from the individual atomic constituents. Scattering from bound electrons is referred to as Rayleigh scattering [14] and dominates the total cross section in a broad energy range from a few keV up to the MeV range. At even higher energies, scattering from vacuum fluctuations in the atomic field (Delbrück scattering [37]) and nuclear scattering [3, 15] become important. Comprehensive reviews on the topic of elastic x-ray scattering by atoms have been given by Kane *et al* [23] in 1986 and Bradley *et al* [5] in 1999.

Recent theoretical investigations of elastic scattering focus on the effects of photon polarization [30, 31, 46, 47, 57, 58]. For all basic photon-matter processes, the features of polarization transfer from the incident to the outgoing beam are of particular importance as they enable tests of theory methods that are more stringent than measuring just total or differential interaction cross sections. Vice versa, with an established theory the incident polarization states of the photons can be reconstructed from the measured polarization of the outgoing photons. However, with respect to Rayleigh scattering, experiments involving (linearly) polarized hard x-rays were up to now restricted to scenarios where either the differential cross section for a linearly polarized incident beam [6, 7, 20, 51, 52] or the polarization of the scattered beam for an unpolarized incident beam [16, 32, 50, 53, 54, 70] was measured. Several of those experiments were compared to theoretical predictions in [44].

For linearly polarized incident x-ray beams a direct measurement of the linear polarization for the outgoing elastically scattered photons was not feasible due to technological limitations: for hard x-ray energies, polarized sources were not intense and polarimeters not efficient enough to compensate for the small elastic scattering cross section, especially at large scattering angles. These difficulties were recently overcome with the advent of third-generation synchrotron radiation facilities and the availability of highly efficient Compton polarimeters. The combination of both instruments now enables scattering experiments with independent determinations of the linear polarizations of the incident and scattered hard x-rays, therefore providing the most stringent test of the theoretical understanding of the underlying processes. Similar experiments were performed recently, where the polarization transfer from spin-polarized electrons to bremsstrahlung photons was investigated [28, 34, 60, 61]. Moreover, these measurements demonstrated that utilizing theoretical estimates of the polarization transfer characteristics enables an accurate reconstruction of the incident beam polarization. As an example, such schemes for polarization diagnostics of particle and photon beams are required for exploring atomic parity violation phenomena [59, 71].

2. Experiment

In this report, we present the first direct measurement of the linear polarization of elastically scattered hard x-rays with a highly linearly polarized incident beam. The experiment was performed at the High Energy Materials Science Beamline P07 [48] of the third-generation synchrotron radiation facility PETRA III at DESY. Details on the setup were discussed in [4], so here we restrict ourselves to briefly describing the main aspects. A gold (high Z) scatterer and a high photon energy of 175 keV were chosen, a regime where Rayleigh scattering is the dominant elastic process and relativistic effects, such as non-vanishing contributions from higher-order multipoles, are predicted to have significant influence. The target was a foil thin enough to neglect multiple-scattering contributions (1.036 μm compared to a mean free path length of the incident photons of 400 μm). A coplanar scattering geometry was chosen, i.e. the scattered photons were observed in the polarization plane of the incident beam. The polarization of the scattered radiation was measured with a thick-crystal, double-sided segmented Si(Li) detector applied as a Compton polarimeter [42, 66], that was placed at polar scattering angles of $\theta = 65°, 90°$ and 120°. This polarimeter consists of a single 7 mm thick lithium-drifted silicon crystal with an active area of 64 mm $\times$ 64 mm which is segmented into 32 strips on the front side and—orthogonal to these—32 strips on the back side. Each of these strips acts as an individual detector with an energy resolution (FWHM) of 2.5 keV at 60 keV. The combination of energy sensitivity with the position resolution of the segmented detector enables one to apply Compton polarimetry, see [68] for a detailed description of the method. This technique for hard x-ray polarization measurements was introduced in the 1950s [38] and was widely used and improved since then, see [29] for a comprehensive overview. Examples for recent Compton polarimetry experiments in the field of atomic physics can be found in [2, 8–10, 13, 22, 49, 60–62] and, in particular with detectors of the type used in the present work, in [18, 19, 33, 34, 69]. Selected experiments on the polarimetry of hard x-rays using thick-crystal, double-sided segmented semiconductor detectors were also recently reviewed in [65].

As an illustration of the analyzed radiation in the current experiment, an energy spectrum of single hits (only one registered photon interaction inside the polarimeter per event, which is in most of the cases related to photoabsorption of the incident photon) is shown in figure 1. Its main features are the characteristic $K\alpha$ and $K\beta$ fluorescence lines from the gold target, the broad Compton peak of inelastically scattered photons and the narrow Rayleigh peak (elastic scattering) at the incident beam energy of 175 keV.

3. Data analysis

For the polarization determination we analyze only double hits (two recorded energy depositions at different positions in the polarimeter per event) as they are candidates for Compton scattering within the detector crystal (one energy deposition being associated to the Compton-scattered photon and the other to the recoil electron). Note that according to the Klein–Nishina equation [27] Compton scattering in the direction perpendicular to the incident photon's electric field vector is preferred, while scattering in the parallel direction is less probable. Thus, the linear polarization characteristics of the x-rays impinging on the detector can be reconstructed from the azimuthal position distribution of Compton-scattered photons inside the detector. As a result of such a polarization study, one usually obtains the degree of linear polarization P_{L} and the orientation φ_0 of the electric field vector (here: with respect to the plane defined by the directions of the initial and Rayleigh-scattered photons) of the analyzed photon beam. A common way to obtain the polarization parameters is to adjust the Klein–Nishina cross section for a photon beam to the measured azimuthal Compton scattering distribution with P_{L} and φ_0 as free parameters. However, for a precise reconstruction of both values it is necessary to take

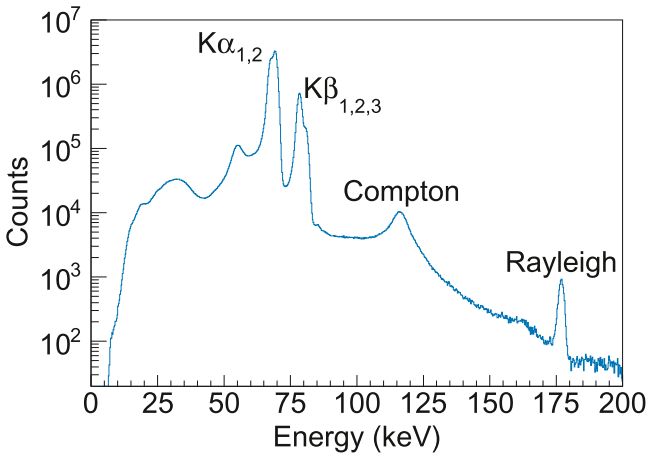

Figure 1. Energy spectrum arising from 175 keV x-rays impinging on a thin gold target, recorded by the polarimeter detector placed at an observation angle of $\theta = 120°$. All prominent features are associated either with fluorescence transitions of the target material or elastic and inelastic scattering in the target foil.

into account geometrical effects resulting from the individual detector characteristics (e. g. the pixel structure) that lead to a deviation of the measured distribution from the ideal behavior of the theoretical cross section. As it was shown in [67], the observed detector response to incident x-rays can be reproduced in great detail when using a Monte Carlo simulation to generate artificial data sets that are processed by the same analysis routine as is used for the experimental data. A possible way to correct for the detector-dependent effects in the scattering distribution is presented in [68], where the measured distribution was normalized to the simulated detector response to unpolarized radiation (i.e. a uniform scattering distribution).

In the present work, we employed a slightly different approach: the measured scattering distribution was fitted with a linear combination of four Monte-Carlo-generated distributions which correspond to the detector response to 100% linearly polarized radiation, oriented in directions of 0°, 45°, 90° and 135° with respect to the reaction plane of the initial scattering in the target foil. Here the intensities I_0, I_{90}, I_{45} and I_{135} were treated as free parameters. Now it is convenient to express the (linear) polarization characteristics of the incident radiation in terms of the corresponding Stokes parameters [36, 55] $P_1 = P_L\cos(2\varphi_0)$ and $P_2 = P_L\sin(2\varphi_0)$. These Stokes parameters follow directly from the intensities I_χ that were obtained in the fitting procedure as $P_1 = (I_0 - I_{90})/(I_0 + I_{90})$ and $P_2 = (I_{45} - I_{135})/(I_{45} + I_{135})$. A bootstrap resampling procedure [11] of the experimental and the Monte Carlo spectra was employed to estimate the statistical uncertainties of P_1 and P_2. Note that for Rayleigh (and Compton) scattering on unpolarized target electrons and scattering in the polarization plane of the incident x-ray beam, the outgoing photon polarization is expected to be oriented perpendicular ($P_1 < 0$) or parallel ($P_1 > 0$) to the scattering plane, resulting in $P_L = |P_1|$ and $P_2 = 0$. To distinguish the (linear) polarization characteristics of the Rayleigh-scattered radiation from the Compton-scattered radiation (both scattering events taking place in the target foil), in the following we shall denote the Stokes parameters of the former with P^R while those for the Compton scattering will be denoted by P^C. Moreover, the linear polarization of the synchrotron radiation impinging on the target foil is denoted by P^i. In order to determine the Stokes parameters P_1^R and P_2^R of the elastically scattered photons from the gold target, in the polarimetry analysis only those events are taken into account where the sum energy of the recoil electron and the Compton-scattered photon (inside the detector) lies in the energy range of the incident photon (chosen here: 173–178 keV, i.e. the Rayleigh peak in figure 1). An example of a measured scattering distribution together with the Monte Carlo fit is shown in figure 2.

4. Results and discussion

The results of the polarization measurement of the Rayleigh-scattered radiation are shown in figure 3. Only P_1^R is plotted because the values for P_2^R are consistent with zero at all observation angles proving that the polarimeter was aligned with the incident beam polarization plane as intended (as a consequence also $P_2^i = 0$). Due to low statistics (compared to previous experiments with the same polarimeter, for example [69]), we considered only statistical uncertainties as they dominate the overall error margin. The comparatively large uncertainty of the $\theta = 90°$ polarization value is due to the fact that the angle-differential Rayleigh cross section has its minimum

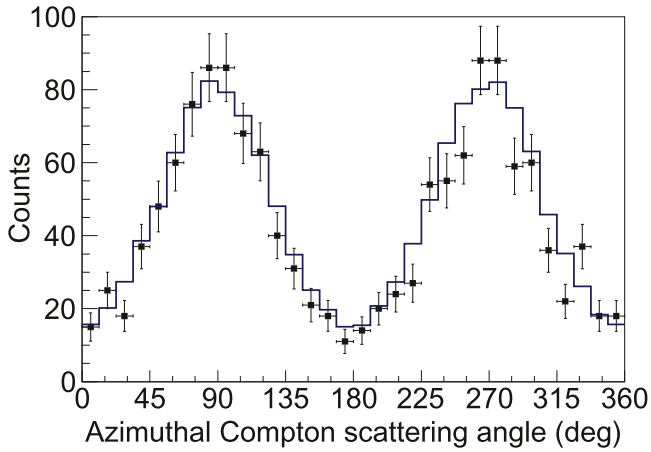

Figure 2. Compton scattering distribution as a function of the azimuthal scattering angle inside the polarimeter detector (placed at $\theta = 65°$). By setting an appropriate energy window, the displayed events are restricted to Rayleigh-scattered photons from the gold target. Data points: experiment, solid line: Monte Carlo simulation adjusted to the experimental data.

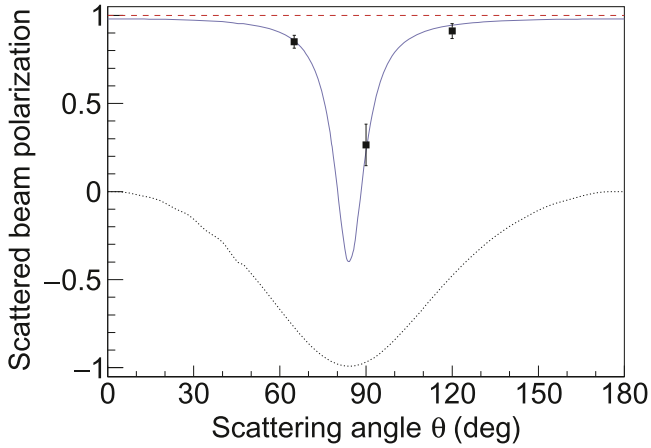

Figure 3. Linear polarization (represented by the Stokes parameter P_1^R) of Rayleigh-scattered 175 keV x-rays from gold in a coplanar geometry as a function of the scattering angle θ. Experimental data points (full squares) are shown together with theories for an incident beam polarization $P_1^i = 0$ (dotted line), $P_1^i = 1$ (dashed line) and $P_1^i = 0.9801$ (solid line). Error bars reflect statistical uncertainties. Predictions are plotted for a point-like detector.

near this observation angle (in coplanar geometry, i.e. scattering along the polarization direction of the incident beam), resulting in an even larger statistical uncertainty.

We observe a strong depolarization of the Rayleigh-scattered radiation in the region near $\theta = 90°$. To explain this finding, we compared our result with fully relativistic (i.e. beyond dipole approximation) theoretical calculations. These have been performed within a Furry picture where the electron–nucleus and (partially) electron–electron interactions are included in the unperturbed Hamiltonian and the coupling to the radiation field is treated perturbatively. In such an approach, all the properties of the Rayleigh scattering can be traced back to the evaluation of the second-order amplitudes [1, 17, 45, 46, 57]. This requires a summation over the *complete* spectrum of the target atom, including not only bound, but also positive and negative energy continuum-states. In order to perform this non-trivial summation over *many-electron* states, we employed the independent particle approximation (IPA) in which the photon is scattered by a single active electron at a time, while the remaining electrons are kept 'frozen' [43, 58]. Such an approximation is known to work fairly well for high-energy photons and heavy targets [41]. In order to partially account for the interaction among the electrons in the target atom, the initial, final and intermediate single-particle states are taken as solutions of the Dirac equation with a screened potential $V_{scr}(r)$, generated within the Dirac–Fock theory. Such a 'screened' IPA model has been successfully applied in the past for the analysis of both Rayleigh scattering [43, 58] and two-photon decay [56] of many-electron atoms and ions. In order to investigate the many-body effects beyond the IPA, we have recently applied the rigorous quantum electrodynamics approach. Based on this approach we have shown that the

Table 1. Stokes parameter P_1^R in % at different scattering angles θ. Theoretical predictions assume a point-like or an extended detector and $P_1^i = +0.9801 \pm 0.0093$.

		Theory	
θ (deg)	Experiment	Point-like	Extended
65	$+85.0 \pm 3.6$	$+85.6 \pm 6.7$	$+81.1 \pm 6.9$
90	$+27 \pm 12$	$+23 \pm 30$	$+10 \pm 25$
120	$+91.2 \pm 4.2$	$+94.5 \pm 2.6$	$+92.8 \pm 3.8$

electron–electron interaction effects do not exceed 3%−4% for both the angular distribution and the linear polarization of the scattered photons [64]. In the angular region of the present experiment ($\theta \geqslant 65°$) we do not expect significant effects which arise from the solid state of the scattering target (compared to the scenario of an isolated atom which is assumed in the theory discussed above). This can be justified by the findings in [58] which indicate that scattering from outer shells (the ones relevant for solid state effects) is only relevant for very small observation angles.

For a theoretical prediction of P_1^R the Stokes parameter P_1^i of the incident PETRA-III beam is required (P_2^i is not needed for coplanar scattering). The synchrotron beam is expected to be nearly 100% linearly polarized, therefore as a first guess we use $P_1^i = 1$ as input for the theoretical calculations. This leads to $P_1^R \approx 1$ (exactly 1 for a closed-shell atom) for all angles (dashed line in figure 3), which clearly deviates from the experimental findings. In our experiment, we were able to independently obtain P_1^i from the measured Stokes parameters P_1^C and P_2^C of the Compton-scattered photons (from the gold target), which are related to the Stokes parameters of the incident beam via the transfer matrix for Compton scattering [12] integrated over the solid angle covered by the active area of the detector. For the scattering angles $\theta = 65°$ and 120° values for P_1^i and P_2^i could be reconstructed, but not for 90° due to a singularity of the transfer matrix at this specific scattering angle. Assuming that the incident beam polarization did not vary during the experiment, we used the weighted mean values of P_1^i and P_2^i as a result. Their errors were conservatively estimated as the maximum difference between the weighted mean and the individual values at both observation angles. With this we obtained $P_1^i = +0.9801 \pm 0.0093$ and $P_2^i = -0.011 \pm 0.019$. The positive P_1^i together with the small value of P_2^i, which agrees with zero, confirms again the initial assumption that the incident beam was polarized in the scattering plane (coplanar geometry). In contrary to the polarization measurement for the Rayleigh-scattered radiation, the uncertainty of the reconstructed polarization of the Compton-scattered x-rays (and consequently also the estimate for P_1^i) is dominated by systematic effects, such as the unknown shape of the background under the broad Compton peak.

For the initial beam polarization $P_1^i = +0.9801$ the corresponding theoretical prediction is depicted by the solid line in figure 3. This theoretical result agrees very well with the experimental data, showing that the strong depolarization of the Rayleigh-scattered photons originates from the polarization impurity of the incident beam. This finding indicates that the polarization of the Rayleigh-scattered beam is highly sensitive to the polarization of the incident beam, especially around $\theta = 90°$. It should be noted that the shown prediction does not take into account the finite detector size, which for each observation angle leads to a (slight) deviation from the values calculated for an infinitely small detector. For completeness, calculations for a point-like and an extended detector with their respective uncertainties are compared with the experimental data in table 1. For the predictions of P_1^R the uncertainty of P_1^i and uncertainties of the observation angles θ and φ ($\pm 1°$ for both) are taken into account. Within the resulting error bars the predictions for a point-like and an extended detector both agree with the experimental data. The large uncertainties in the predictions at $\theta = 90°$ are due to the previously found high sensitivity of P_1^R to P_1^i, which magnifies the uncertainty resulting from ΔP_1^i.

In order to explain this high sensitivity, it is convenient to decompose the incident beam into beams of photons which are polarized parallel and perpendicular to the scattering plane. These portions of the beam are scattered independently from each other with amplitudes $A_\parallel$ and $A_\perp$, respectively. In the form factor approximation, one has $A = A_\perp \cos(\theta)$ [26], so that $A_\parallel$ vanishes at $\theta = 90°$, i.e. coplanar scattering is strictly forbidden at that angle (perfect polarization filter). In fully relativistic S-matrix calculations $A_\parallel$ is finite at all angles [58], but around $\theta = 90°$, one still has $|A| \ll |A_\perp|$ [21] (almost perfect polarization filter). Therefore even a small admixture of perpendicularly polarized photons in the incident beam can lead to a large fraction of perpendicularly polarized photons in the scattered beam at 90° and therefore to the pronounced depolarization and polarization sensitivity that were observed. In angular regions away from $\theta = 90°$ the effect is weaker because $|A|$ and $|A_\perp|$ are of the same order. In figure 4, P_1^R is shown as a function of P_1^i for the scattering angles covered in the present experiment. The sensitivity can be directly identified with the derivative and it is clearly highest for $\theta = 90°$ and $P_1^i \to +1$.

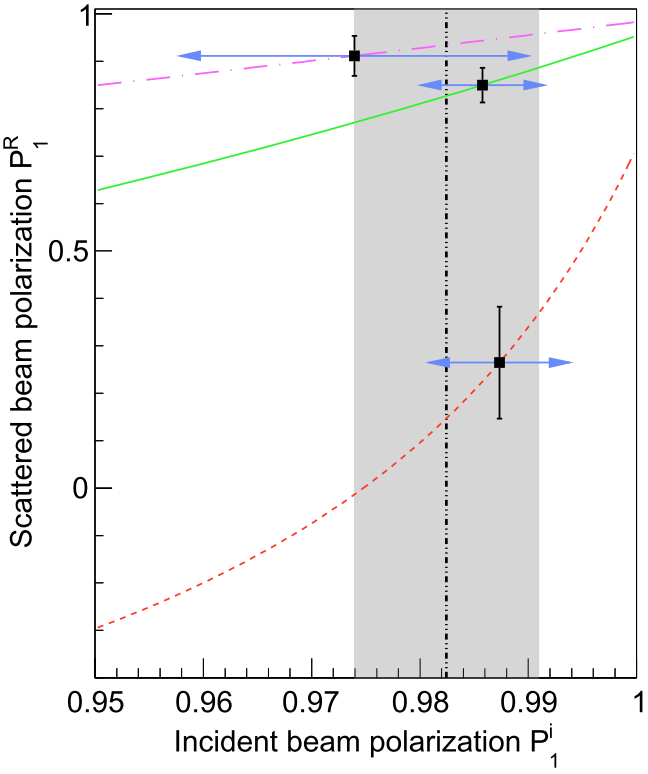

Figure 4. Linear polarization of Rayleigh-scattered 175 keV x-rays as a function of the incident beam polarization for different scattering angles $\theta = 65°$ (solid line), 90° (dashed line) and 120° (dash–dotted line). Data points are the measured P_1^R versus the corresponding reconstructed P_1^i. The uncertainties of P_1^i introduced by this reconstruction—which mainly arise from the uncertainty of P_1^R, but also from the geometry—are indicated by the arrows. Vertical dash-double-dotted line with filled area: weighted mean of reconstructed P_1^i with its uncertainty. Unlike in figure 3, here the predictions are shown for an extended detector as was used in the present experiment.

The reader might note, that the pronounced difference in the magnitude of the Rayleigh scattering amplitudes near 90° leads to a significant increase of the scattering intensity when the incident beam linear polarization deviates from 100%. Thus, it would be possible to infer a possible polarization impurity from a deviation of the measured cross section at observation angles near 90°. However, obtaining absolute cross sections is a challenging task that is often hampered by uncertainties of incident beam flux, target thickness, detector efficiency, covered solid angle, etc so that typically uncertainties are of the order of 30% or more. In contrast, the determination of the linear polarization of the Rayleigh-scattered photons boils down to the analysis of the emission pattern of Compton scattering inside the detector crystal, i.e. a relative measurement that is unaffected by the systematic uncertainties mentioned above. Nevertheless, we plan to perform cross section measurements of polarization-dependent Rayleigh scattering as a follow-up study to the present work.

While the high sensitivity makes it difficult to predict P_1^R, it can be exploited when the theory is applied inversely, i.e. when P_1^i is reconstructed from the measured P_1^R. In such a procedure, a high sensitivity allows to determine P_1^i very precisely, even though the uncertainty of P_1^R is relatively large. The results for the reconstruction of P_1^i in the present experiment are also shown in figure 4. Of all the angles covered in the present experiment, the sensitivity is lowest at $\theta = 120°$, resulting in the largest uncertainty of the reconstructed P_1^i. At 65° and 90°, these uncertainties are comparable, even though the sensitivity is significantly higher at 90° where the uncertainty of the measured P_1^R is larger. The latter has two reasons: firstly, the statistics were lowest at 90°. Secondly, a significantly smaller (absolute) value of P_1^R needed to be measured (for a given number of events, the statistical uncertainty of Compton polarimetry increases when the degree of polarization decreases [40]). The reconstructed values of P_1^i at the three angles agree with each other and their weighted mean, $+0.9824 \pm 0.0085$, which also agrees with the value derived from the linear polarization of the Compton-scattered photons. It is important to note that the precision of the P_1^i estimate based on Rayleigh scattering could be significantly increased by accumulating more statistics. In the present measurement the amount of recorded data was limited by the count rate of the polarimeter detector that could be handled by the data acquisition system (based on NIM and VME modules). We expect that a fully digital readout of the detector will enable a ten times higher count rate (about 10 kHz) which for the present experimental parameters would result in a very small uncertainty of the reconstructed synchrotron beam polarization close to 0.25%.

5. Conclusion and outlook

In summary, the polarization transfer in Rayleigh scattering of highly linearly polarized hard x-rays was studied at the synchrotron radiation source PETRA III. We observed a significant depolarization of the scattered photons at scattering angles close to $\theta = 90°$ which is in agreement with fully relativistic calculations when taking into account a small polarization impurity of the incident photon beam. Indeed, an imperfect linear polarization of about 98% was obtained independently from the Rayleigh measurement by analyzing the polarization of the Compton-scattered radiation from the target. Thus, the present experiment enabled a very stringent test of polarization transfer theory in Rayleigh scattering, as both the polarization features of the incident and the outgoing radiation were obtained for the first time.

This strong polarization sensitivity makes Rayleigh scattering a very promising candidate for precision polarization diagnostics for highly polarized photon beams (e.g. at synchrotron facilities) considering the following advantages: only a thin, passive target needs to be placed in the primary beam. Moreover, from tabulated *S*-matrix amplitudes [24, 25] we estimate that the observed polarization sensitivity is sufficiently pronounced at least over the entire range of incident photon energies where the applied model is valid, i.e. well above the *K*-shell ionization threshold of the target (to justify IPA) and below energies where the Delbrück amplitude is non-negligible (differential cross section data are described well without the Delbrück amplitude up to 662 keV [39]). One could also use the polarization of the Compton-scattered photons to reconstruct the incident beam polarization. In the present experiment, this method yielded a comparable accuracy as with the Rayleigh-scattered photons, even though the statistics for the Compton-scattered photons were significantly higher. We expect that Rayleigh scattering is the more suitable of the two processes for polarization diagnostics, as it features a monoenergetic peak which simplifies the background estimation in comparison to the broad Compton profile. Furthermore, in the mentioned range where Rayleigh scattering provides sufficient polarization sensitivity, Compton scattering rapidly looses sensitivity when the photon energy is increased. For lower photon energies, other polarization diagnostic schemes can be applied, for example a Compton polarimeter with a passive scatterer mounted directly in the synchrotron radiation beam was reported in [63] for the energy range of 15–40 keV. Below 20 keV, extremely polarization-sensitive channel-cut crystals can be employed [35]. We see Rayleigh scattering as a complement to the mentioned techniques as it covers higher energies (>100 keV).

Acknowledgments

The support of Max Schwemlein and Thorsten Groß is acknowledged. Parts of this research were carried out at the light source PETRA III at DESY, a member of the Helmholtz Association (HGF). VAY acknowledges support by Russian Foundation for Basic Research (grant No. 16-02-00538).

References

[1] Akhiezer A I and Berestetskii V B 1965 *Quantum Electrodynamics vol XI of Interscience Monographs and Texts in Physics and astronomy* (New York: Interscience)
[2] Beilicke M *et al* 2015 First flight of the x-ray polarimeter X-Calibur *2015 IEEE Aerospace Conf.* pp 1–10
[3] Berant Z, Moreh R and Kahane S 1977 Nuclear thomson scattering of 5.5–7.2 MeV photons *Phys. Lett.* B **69** 281–3
[4] Blumenhagen K-H, Spillmann U, Gassner T, Gumberidze A, Märtin R, Schell N, Trotsenko S, Weber G and Stöhlker T 2015 Identification and reduction of unwanted stray radiation using an energy- and position-sensitive Compton polarimeter *Phys. Scr.* **T166** 014032
[5] Bradley D A, Gonçalves O D and Kane P P 1999 Measurements of photon-atom elastic scattering cross-sections in the photon energy range 1 KeV–4 MeV *Radiat. Phys. Chem.* **56** 125–50
[6] Brini D, Fuschini E, Murty D S R and Veronesi P 1959 Rayleigh scattering of polarized photons *Il Nuovo Cimento* **11** 533–45
[7] Brini D, Fuschini E, Peli L and Veronesi P 1958 Elastic scattering of polarized photons *Il Nuovo Cimento* **7** 877–90
[8] Chauvin M *et al* 2016 Observation of polarized hard x-ray emission from the Crab by the PoGOLite Pathfinder *Mon. Not. R. Astron. Soc.: Lett.* **456** L84–8
[9] Chauvin M, Roques J P, Clark D J and Jourdain E 2013 Polarimetry in the hard x-ray domain with integral SPI *Astrophys. J.* **769** 137
[10] Dean A J, Clark D J, Stephen J B, McBride V A, Bassani L, Bazzano A, Bird A J, Hill A B, Shaw S E and Ubertini P 2008 Polarized gamma-ray emission from the Crab *Science* **321** 1183–5
[11] Efron B 1979 Bootstrap methods: another look at the jackknife *Ann. Stat.* **7** 1–26
[12] Fano U 1949 Remarks on the classical and quantum-mechanical treatment of partial polarization *J. Opt. Soc. Am.* **39** 859
[13] Forot M, Laurent P, Grenier I A, Gouiffès C and Lebrun F 2008 Polarization of the Crab pulsar and nebula as observed by the *INTEGRAL/IBIS* telescope *Astrophys. J.* **688** L29–32
[14] Franz W 1935 Rayleighsche Streuung harter Strahlung an schweren Atomen *Z. Phys.* **98** 314–20
[15] Fuller E G and Hayward E 1962 The nuclear photoeffect in holmium and erbium *Nucl. Phys.* **30** 613–35
[16] Fuschini E, Murty D S R and Veronesi P 1960 Polarization effects in the elastic scattering of photons *Il Nuovo Cimento* **15** 847–9
[17] Gavrila M 1967 Elastic scattering of photons by a hydrogen atom *Phys. Rev.* **163** 147–55
[18] Hess S *et al* 2009 Polarization studies of radiative electron capture into highly-charged uranium ions *J. Phys.: Conf. Ser.* **163** 012072

[19] Hess S *et al* 2009 Polarized tunable monoenergetic x-rays produced by radiative electron capture into the *K*-shell of Xe^{54+} *J. Phys.: Conf. Ser.* **194** 012025
[20] Ice G E, Chen M H and Crasemann B 1978 Photon-scattering cross sections of H_2 and He measured with synchrotron radiation *Phys. Rev.* A **17** 650–8
[21] Johnson W R and Cheng K-t 1976 Elastic scattering of 0.1–1 MeV photons *Phys. Rev.* A **13** 692–8
[22] Jörg H, Hu Z, Bekker H, Blessenohl M A, Hollain D, Fritzsche S, Surzhykov A, López-Urrutia J R C and Tashenov S 2015 Linear polarization of x-ray transitions due to dielectronic recombination in highly charged ions *Phys. Rev.* A **91** 042705
[23] Kane P P, Kissel L, Pratt R H and Roy S C 1986 Elastic scattering of γ-rays and x-rays by atoms. *Phys. Rep.* **140** 75–159
[24] Kissel L RTAB: Rayleigh scattering database (http://starship.org/RTAB/RTAB.php)
[25] Kissel L 2000 RTAB: the Rayleigh scattering database *Radiat. Phys. Chem.* **59** 185–200
[26] Kissel L, Pratt R H and Roy S C 1980 Rayleigh scattering by neutral atoms, 100 eV–10 MeV *Phys. Rev.* A **22** 1970–2004
[27] Klein O and Nishina Y 1929 Über die Streuung von Strahlung durch freie Elektronen nach der neuen relativistischen Quantendynamik von Dirac *Z. Phys.* **52** 853–68
[28] Kovtun O, Tioukine V, Surzhykov A, Yerokhin V A, Cederwall B and Tashenov S 2015 Spin–orbit interaction in bremsstrahlung and its effect on the electron motion in a strong Coulomb field *Phys. Rev.* A **92** 062707
[29] Lei F, Dean A J and Hills G L 1997 Compton polarimetry in gamma-ray astronomy *Space Sci. Rev.* **82** 309–88
[30] Manakov N L, Meremianin A V, Carney J P J and Pratt R H 2000 Circular dichroism effects in atomic x-ray scattering *Phys. Rev.* A **61** 032711
[31] Manakov N L, Meremianin A V, Maquet A and Carney J P J 2000 Photon-polarization effects and their angular dependence in relativistic two-photon bound-bound transitions *J. Phys. B: At. Mol. Opt. Phys.* **33** 4425–46
[32] Manuzio G and Vitale S 1961 Diffusione elastica di raggi γ di 1.25 MeV in piombo *Il Nuovo Cimen* **20** 638–47
[33] Märtin R, Weber G, Barday R, Fritzsche Y, Enders J, Spillmann U and Stöhlker T 2013 Target-thickness effects in electron-atom bremsstrahlung *Phys. Scr.* **T156** 014070
[34] Märtin R *et al* 2012 Polarization transfer of bremsstrahlung arising from spin-polarized electrons *Phys. Rev. Lett.* **108** 264801
[35] Marx B *et al* 2013 High-precision x-ray polarimetry *Phys. Rev. Lett.* **110** 254801
[36] McMaster W H 1961 Matrix representation of polarization *Rev. Mod. Phys.* **33** 8–28
[37] Meitner L and Kösters H 1933 Über die Streuung kurzwelliger γ-Strahlen *Z. Phys.* **84** 137–44
[38] Metzger F and Deutsch M 1950 A study of the polarization-direction correlation of successive gamma-ray quanta *Phys. Rev.* **78** 551–8
[39] Milstein A I and Schumacher M 1994 Present status of delbrück scattering *Phys. Rep.* **243** 183–214
[40] Montgomery C G and Swank J H 2015 Statistics of x-ray polarization measurements *Astrophys. J.* **801** 21
[41] Pratt R H 2004 Tutorial on fundamentals of radiation physics *Radiat. Phys. Chem.* **70** 595–603
[42] Protić D, Hull E L, Krings T and Vetter K 2005 Large-volume Si Li orthogonal-strip detectors for Compton-effect-based instruments *IEEE Trans. Nucl. Sci.* **52** 3181–5
[43] Roy S C, Kissel L and Pratt R H 1999 Elastic scattering of photons *Radiat. Phys. Chem.* **56** 3–26
[44] Roy S C, Sarkar B, Kissel L D and Pratt R H 1986 Polarization effects in elastic photon-atom scattering *Phys. Rev.* A **34** 1178–87
[45] Safari L, Amaro P, Fritzsche S, Santos J P and Fratini F 2012 Relativistic total cross section and angular distribution for Rayleigh scattering by atomic hydrogen *Phys. Rev.* A **85** 043406
[46] Safari L, Amaro P, Fritzsche S, Santos J P, Tashenov S and Fratini F 2012 Relativistic polarization analysis of Rayleigh scattering by atomic hydrogen *Phys. Rev.* A **86** 043405
[47] Safari L, Amaro P, Santos J P and Fratini F 2015 Spin effects probed by Rayleigh x-ray scattering off hydrogenic ions *Radiat. Phys. Chem.* **106** 271–7
[48] Schell N, King A, Beckmann F, Fischer T, Müller M and Schreyer A 2013 The high energy materials science beamline HEMS at PETRA III *Mater. Sci. Forum* **772** 57–61
[49] Shah C *et al* 2015 Polarization measurement of dielectronic recombination transitions in highly charged krypton ions *Phys. Rev.* A **92** 042702
[50] Singh M and Sood B S 1965 Measurements of the linear polarization of elastically scattered gamma rays *Nucl. Phys.* **64** 502–12
[51] Smend F, Schaupp D, Czerwinski H, Schumacher M, Millhouse A H and Kissel L 1987 Large-angle Rayleigh scattering of linearly polarized, hard synchrotron x rays by krypton and xenon *Phys. Rev.* A **36** 5189–99
[52] Somayajulu D R S and Lakshminarayana V 1968 Rayleigh scattering of polarized photons *J. Phys. A: Gen. Phys.* **1** 228–35
[53] Somayajulu D R S, Rama Rao J and Lakshminarayana V 1968 Polarization of elastically scattered gamma rays *Il Nuovo Cimento* B **10** 281–92
[54] Sood B S 1958 Polarization of 0.411, 0.662 and 1.25 MeV γ-Rays elastically scattered by lead *Proc. R. Soc.* A **247** 375–80
[55] Stokes G G 1852 On the composition and resolution of streams of polarized light from different sources *Trans. Camb. Phil. Soc.* **9** 399 (http://adsabs.harvard.edu/abs/1851TCaPS...9..399S)
[56] Surzhykov A, Pratt R H and Fritzsche S 2013 Two-photon decay of inner-shell vacancies in heavy atoms *Phys. Rev.* A **88** 042512
[57] Surzhykov A, Yerokhin V A, Jahrsetz T, Amaro P, Stöhlker T and Fritzsche S 2013 Polarization correlations in the elastic Rayleigh scattering of photons by hydrogenlike ions *Phys. Rev.* A **88** 062515
[58] Surzhykov A, Yerokhin V A, Stöhlker T and Fritzsche S 2015 Rayleigh x-ray scattering from many-electron atoms and ions *J. Phys. B: At. Mol. Opt. Phys.* **48** 144015
[59] Surzhykov A, Fritzsche S, Stöhlker T and Tashenov S 2005 Application of radiative electron capture for the diagnostics of spin-polarized ion beams at storage rings *Phys. Rev. Lett.* **94** 203202
[60] Tashenov S *et al* 2013 Bremsstrahlung polarization correlations and their application for polarimetry of electron beams *Phys. Rev.* A **87** 022707
[61] Tashenov S, Bäck T, Barday R, Cederwall B, Enders J, Khaplanov A, Poltoratska Y, Schässburger K-U and Surzhykov A 2011 Measurement of the correlation between electron spin and photon linear polarization in atomic-field bremsstrahlung *Phys. Rev. Lett.* **107** 173201
[62] Tashenov S *et al* 2006 First measurement of the linear polarization of radiative electron capture transitions *Phys. Rev. Lett.* **97** 223202
[63] Tokanai F, Sakurai H, Gunji S, Motegi S, Toyokawa H, Suzuki M, Hirota K, Kishimoto S and Hayashida K 2004 Hard x-ray polarization measured with a Compton polarimeter at synchrotron radiation facility *Nucl. Instrum. Methods Phys. Res.* A **530** 446–52
[64] Volotka A V, Yerokhin V A, Surzhykov A, Stöhlker T and Fritzsche S 2016 Many-electron effects on x-ray Rayleigh scattering by highly charged He-like ions *Phys. Rev.* A **93** 023418
[65] Weber G *et al* 2015 Compton polarimetry using double-sided segmented x-ray detectors *J. Phys.: Conf. Ser.* **583** 012041

[66] Weber G, Bräuning H, Hess S, Märtin R, Spillmann U and Stöhlker T 2010 Performance of a position sensitive Si Li x-ray detector dedicated to Compton polarimetry of stored and trapped highly-charged ions *J. Instrum.* **5** C07010
[67] Weber G, Bräuning H, Märtin R, Spillmann U and Stöhlker T 2011 Monte Carlo simulations for the characterization of position-sensitive x-ray detectors dedicated to Compton polarimetry *Phys. Scr.* **T144** 014034
[68] Weber G *et al* 2015 Combined linear polarization and angular distribution measurements of x-rays for precise determination of multipole-mixing in characteristic transitions of high-Z systems *J. Phys. B: At. Mol. Opt. Phys.* **48** 144031
[69] Weber G *et al* 2010 Direct determination of the magnetic quadrupole contribution to the Lyman-α_1 transition in a hydrogenlike ion *Phys. Rev. Lett.* **105** 243002
[70] Williams R A and McNeill K G 1965 Polarization of elastically scattered 1.33 MeV photons *Can. J. Phys.* **43** 1078–87
[71] Zaytsev V A, Tashenov S, Maiorova A V, Shabaev V M and Stöhlker T 2015 Parity nonconservation effect in the resonance elastic electron scattering on heavy He-like ions *J. Phys. B: At. Mol. Opt. Phys.* **48** 165003